Express Polymer Letters Vol.20, No.9 (2026) 923–938
Available online at www.expresspolymlett.com
https://doi.org/10.3144/expresspolymlett.2026.68

Research article

From ground tire rubber to thermoplastic dynamic vulcanizates: Tailoring high-recycled-content TPU compounds by devulcanization and dynamic vulcanization

Andrea Kohári, *Tamás Bárány**

Department of Polymer Engineering, Faculty of Mechanical Engineering, Budapest University of Technology and Economics, Műegyetem rkp. 3., H-1111 Budapest, Hungary

Received 15 July 2026; accepted in revised form 14 August 2026

Abstract. The virgin polymer content of thermoplastic polyurethane (TPU) can be reduced with the use of recycled tire rubber, but blend properties strongly depend on the structure of the rubber phase. In this study, we compared TPU-based compounds containing ground tire rubber (GTR), devulcanized GTR (dGTR) and dynamically revulcanized dGTR in terms of mechanical and rheological behavior. GTR-filled blends showed higher tensile strength at the same rubber content, whereas dGTR-containing blends exhibited higher elongation at break up to 40 wt% rubber. Among the thermoplastic dynamic vulcanizates, peroxide-cured blends provided higher tensile strength, higher elongation at break and lower compression set than sulfur-cured blends. The rubber phase also strongly affected melt rheology: dGTR-containing blends showed higher storage modulus (G') and complex viscosity (η^*) than the corresponding GTR-filled blends over the entire frequency range. In contrast, there were only minor rheological differences between sulfur- and peroxide-cured systems, indicating that rubber content had a stronger effect on melt behavior than the curing system. The novelty of this study is the direct comparison of GTR, dGTR and dynamically revulcanized dGTR within the same TPU matrix, showing how the breakdown and partial rebuilding of the recycled rubber network can be used to tune both solid-state properties and melt processability in TPU compounds with high recycled content.

Keywords: *recycling, ground tire rubber, devulcanization, revulcanization, thermoplastic polyurethane, thermoplastic elastomers*

1. Introduction

More than one billion tires reach the end of their service life every year, creating a large and continuously growing waste stream worldwide. Tire rubber has a permanently crosslinked structure and a complex composition, which prevents its reprocessing with conventional thermoplastic technologies. Material recycling is therefore often based on mechanical size reduction to produce ground tire rubber (GTR), which can be incorporated into various polymer matrices [1–3]. GTR contains valuable materials, including elastomers, carbon black, processing oils and other additives, but its use in high-value applications is still limited. The crosslinked rubber particles have limited deformability and usually form weak interactions with thermoplastic matrices. As a result, increasing GTR content often reduces tensile strength, elongation at break and fracture resistance [4–6].

Thermoplastic polyurethane (TPU) is an attractive matrix for recycled tire rubber. Its soft and hard segments form a microphase-separated structure that gives TPU a combination of elasticity, toughness, abrasion resistance and melt processability [7, 8]. The difference in modulus between TPU and tire rubber is also smaller than between GTR and common

*Corresponding author, e-mail: barany.tamas@gpk.bme.hu

polyolefins such as polyethylene or polypropylene. This may reduce stress concentration around the rubber particles and allow relatively high GTR contents while the blends retain their elastomeric character. However, the interaction between TPU and GTR remains limited. Particle debonding, cavitation and pull-out can occur during mechanical loading and lead to early failure of the blends [9–11].

Devulcanization offers a possible way to change the structure of recycled tire rubber. The main purpose of devulcanization is to break sulfur-containing crosslinks while limiting polymer chain scission. A decrease in crosslink density increases rubber chain mobility and improves processability [12, 13]. Changes in the rubber network and surface may also affect the interaction between the rubber phase and the thermoplastic matrix. However, crosslink cleavage and polymer chain scission usually occur simultaneously. The balance between these processes strongly affects the properties of devulcanized ground tire rubber (dGTR) and its blends [14].

The partially broken network of dGTR also allows the rubber phase to be vulcanized again. During dynamic vulcanization, crosslinking occurs within a molten thermoplastic matrix under shear. The rubber phase is crosslinked and dispersed into particles, while the thermoplastic phase remains the continuous phase. The resulting thermoplastic dynamic vulcanizates (TDV) combine rubber-like behavior with thermoplastic processability [15, 16]. These materials are usually prepared from virgin rubber, but dGTR can also be used as the rubber phase because its modified network can form new crosslinks [17–19]. The dynamic vulcanization of dGTR may therefore offer a new way to control the properties of TPU blends with high recycled rubber content.

TPU/GTR blends, devulcanized tire rubber and thermoplastic dynamic vulcanizates have been studied previously in several studies, but they are usually investigated separately [9, 10, 20]. There are not many direct comparisons of GTR, dGTR and dynamically vulcanized dGTR within the same TPU matrix and under the same processing and testing conditions. Therefore, the effect of the structure of recycled tire rubber on the mechanical and rheological properties of TPU blends remains incompletely understood. In particular, limited information is available on how the partial breakdown and subsequent rebuilding of the rubber network affect blends with increasing rubber content.

Our goal was to compare TPU blends containing GTR, dGTR and dynamically vulcanized dGTR within the same material platform and under the same processing and testing conditions. We varied rubber content from 30 to 60 wt% to compare the different rubber phases across a wide composition range, and characterized the network structure and vulcanization behavior of the rubber phases first. We then studied the mechanical properties and melt rheology of the TPU blends as a function of rubber content. Sulfur- and peroxide-based vulcanization systems were also compared for the dynamic vulcanization of dGTR. Our main goal was to understand how the amount and structure of recycled tire rubber affect the properties of TPU-based blends and to evaluate dynamic vulcanization as a route for the high-value use of end-of-life tire rubber.

2. Materials and methods

2.1. Materials

We selected a polyether-based thermoplastic polyurethane, Elastollan 1170 A 10 000 (BASF, Mannheim, Germany), as the matrix polymer for the investigated blends. Ground tire rubber (GTR) and devulcanized ground tire rubber (dGTR), both derived from end-of-life truck tires, were supplied by Tyromer Inc. (Arnhem, Netherlands). According to the manufacturer, the dGTR was produced via a thermomechanical devulcanization process assisted by supercritical carbon dioxide. According to the manufacturer's data sheet, the Mooney viscosity (ML, 1+4, 100 °C) of dGTR was 45 ± 15 MU. The GTR had a particle size of less than 2 mm, with an average particle size of 610 ± 7 μm. Table 1 contains the other additives incorporated into the rubber compounds.

2.2. Preparation

Before processing, the TPU pellets and all prepared compounds were dried in a Baxter DN-63 hot-air oven (Baxter Inc., Glenview, USA) at 80 °C for 12 h, which eliminated absorbed moisture, as thermoplastic polyurethane is highly susceptible to moisture uptake. Because of their manufacturing process, both the GTR and the dGTR also had considerable moisture content and were therefore subjected to the same drying procedure before compounding.

Table 1. Additives used in the rubber compounds.

Material	Manufacturer	Trademark	Function
Zinc oxide	Werco Metal (Zlatna, Romania)	–	Activator
Stearic acid	Oleon (Ertvelde, Belgium)	Radiacid 0154	Activator
N-cyclohexyl-2-benzothiazolesulfenamide (CBS)	Rhein Chemie (Mannheim, Germany)	Rhenogran CBS-80	Accelerator
Tetramethyl thiuram disulfide (TMTD)	Lanxess (Mannheim, Germany)	Rhenogran TMTD-70	Accelerator
Sulfur	Ningbo Actmix Polymer (Ningbo, Zhejiang, China)	ACTMIX S-80	Curing agent
1,4-butanediol dimethacrylate (BDMA)	Lanxess (Mannheim, Germany)	Rhenofit BDMA/S	Coagent
Di-(2-tert-butyl-peroxyisopropyl)-benzene (DIPP)	Pergan GmbH (Bocholt, Germany)	Peroxan BIB-40 EV-G	Curing agent

The rubber compounds (dGTR-S and dGTR-P) were prepared with a Brabender Plasti Corder internal mixer (Brabender GmbH, Duisburg, Germany) equipped with a 370 cm^3 mixing chamber (W 350 E). Mixing was carried out at 50 °C, with a rotor speed of 40 rpm and lasted for 10 min. The formulation of dGTR-based rubber compounds for dynamic vulcanization was selected based on our previously published optimization study (Table 2) [21].

Contrary to standard practice, when calculating the formulation of rubber compounds, we assumed that dGTR, as a rubber, was 167 phr rather than 100 phr. The reason for this is that, based on thermogravimetric analysis (see Section 3.1), dGTR contained approximately 60 wt% elastomer.

Two-millimeter-thick vulcanized rubber sheets were prepared by compression molding between polytetrafluoroethylene-coated metal plates. Vulcanization was carried out at 180 °C under 2.8 MPa with the use of the optimal vulcanization time (t_{90}), determined for each compound. Molding was performed with a Teach-Line Platen Press 200E hydraulic press (Dr. Collin GmbH, Ebersberg, Germany).

TPU-based blends containing different rubber phases were compounded with a co-rotating twin-screw extruder (LTE 26-44, Labtech Scientific, Labtech Engineering Co., Ltd., Samutprakarn, Thailand) equipped with 26 mm diameter screws and an *L*/*D* ratio of 44. During processing, barrel temperature was gradually increased from 155 °C in the feeding section to 190 °C at the die according to the following profile: 155–155–160–160–165–170–175–180–185–190–190 °C. The rotation speed of the screw was maintained at 120 rpm throughout the extrusion process.

Before melt compounding, the TPU pellets were dry-mixed with GTR, dGTR, or the corresponding rubber compounds for a homogeneous feedstock. The resulting dry mixture was subsequently introduced into the extruder through the hopper. Table 3 shows the formulations investigated in this study.

Square, 2 mm thick, 80×80 mm plates were manufactured from the prepared blends with an Arburg Allrounder Advance 270S 400-170 injection molding machine (Arburg GmbH, Lossburg, Germany). Table 4 shows the processing conditions applied during injection molding. All specimens used for subsequent characterization were cut from the injection molded plates.

Table 2. Recipes for the rubber compounds (phr: parts per hundred rubber).

Material	Amount of ingredients [phr]	
	dGTR-S	dGTR-P
dGTR	167.0	167.0
Zinc oxide	5.0	–
Stearic acid	2.0	–
CBS	1.5	–
TMTD	0.5	–
Sulfur	1.0	–
BDMA	–	1.0
DIPP	–	2.5

Table 3. The composition of the blends.

Compound	Components
TPU/GTR_X	(100-X) wt% TPU + X wt% GTR
TPU/dGTR_X	(100-X) wt% TPU + X wt% dGTR
TPU/dGTR-S_X	(100-X) wt% TPU + X wt% dGTR-S
TPU/dGTR-P_X	(100-X) wt% TPU + X wt% dGTR-P

Table 4. Injection molding parameters.

Parameter		Value
Melt temperature	[°C]	210
Injection rate	[cm^3/s]	50
Dose volume	[cm^3]	45
Holding pressure	[bar]	450
Holding time	[s]	15
Residual cooling time	[s]	30
Mold temperature	[°C]	30

TDV compounds containing 60 wt% rubber were not included in the study because, at this loading, the dynamically vulcanized systems showed insufficient melt processability and could not be reproducibly injection molded into defect-free specimens with the applied processing conditions. Therefore, the rubber content of the TDV series was limited to 50 wt%, whereas the non-vulcanized GTR and dGTR blends were successfully processed up to 60 wt%.

2.3. Characterization methods

The thermogravimetric analysis (TGA) of GTR and dGTR was performed with a TA Q500 instrument (TA Instruments Ltd., New Castle, USA) in a nitrogen atmosphere at a heating rate of 10 °C/min between 50 and 600 °C. To determine carbon black content, we switched to an air atmosphere at 600 °C and heated the sample at a rate of 10 °C/min to 800 °C. The reported results are based on the average of three measurements.

The crosslink density of the rubber phases was evaluated with the equilibrium swelling method. The specimens were immersed in toluene at room temperature for 72 h to reach swelling equilibrium. After removal from the solvent, the samples were gently blotted with paper towels, and the swollen mass was recorded. Subsequently, the specimens were dried at 80 °C for 12 h, and their final dry mass was measured. Crosslink density was calculated according to the Flory-Rehner equation (Equation (1)):

$$\nu_e = \frac{-\left[\ln(1-V_r) + V_r + \chi \cdot V_r^2\right]}{V_s \cdot \left(V_r^{\frac{1}{3}} - \frac{V_r}{2}\right)} \quad (1)$$

where ν_e is crosslink density [mol/cm^3], V_s is the molar volume of toluene (106.27 cm^3/mol), χ is the Flory-Huggins polymer–solvent interaction parameter, taken as 0.39 [22], and V_r is the volume fraction of rubber in the swollen network. The value of V_r was determined with the Ellis-Welding equation (Equation (2)):

$$V_r = \frac{\frac{m_r}{\rho_r}}{\frac{m_r}{\rho_r} + \frac{m_s}{\rho_s}} \quad (2)$$

where m_r is the mass of the dried rubber sample, m_s is the mass of solvent absorbed during swelling, ρ_r is the density of the rubber sample, and ρ_s is the density of toluene, taken as 0.867 g/cm^3 [23, 24]. The reported crosslink density values are the average of those of five specimens.

The soluble fraction of the samples was determined by Soxhlet extraction with toluene as the solvent. The extraction was carried out in boiling toluene for 16 h. After extraction and drying, the soluble content (S) was calculated according to Equation (3):

$$S = \left(1 - \frac{m_f}{m_i}\right) \cdot 100\% \quad (3)$$

where m_i and m_f denote the initial mass of the sample before extraction and the final mass after extraction, respectively. The reported soluble fraction values are the average of those of five specimens.

The vulcanization behavior of the rubber compounds was characterized with a MonTech D RPA 3000 Rubber Process Analyzer (MonTech GmbH, Buchen, Germany). Measurements were performed under isothermal (180 °C) and non-isothermal conditions (155–190 °C at a heating rate of 17.5 °C/min), with a testing frequency of 1.67 Hz and a strain amplitude of 1°. The characteristic vulcanization parameters were determined in accordance with ISO 6502-2:2018. Scorch time (t_{10}) was defined as the time required to reach 10% of total cure, while vulcanization time (t_{90}) corresponded to the time required for 90% of total cure. In addition, the torque difference ($\Delta S' = S'_{max} - S'_{min}$) was calculated, where S'_{max} and S'_{min} represent the maximum and minimum torque, respectively. This parameter was used as an indicator of changes in the crosslink density of the rubber compounds. The cure rate index (CRI), which characterizes the rate of vulcanization, was calculated according to Equation (4).

$$CRI = \frac{100}{t_{90} - t_{10}} \quad (4)$$

where t_{10} and t_{90} are expressed in min.

The tensile properties of the specimens were evaluated with a Zwick Z005 universal testing machine

(Zwick GmbH, Ulm, Germany) equipped with a 5 kN load cell. Tensile tests were carried out at room temperature in accordance with ISO 37:2017 with the use of Type 2 dumbbell-shaped specimens. Crosshead speed was set to 500 mm/min, while initial gauge length was 45 mm. Five parallel specimens were tested for each composition and the measured values were averaged.

The effects of rubber type or vulcanization system and rubber content on tensile strength and elongation at break were evaluated by two-way analysis of variance (ANOVA), followed by Tukey's post hoc test at a significance level of $p < 0.05$.

The Shore A hardness of the samples was measured with a Zwick H04.3150.000 hardness tester (Zwick GmbH, Ulm, Germany) in accordance with ISO 7619-1:2010 at 10 points per sample. The total thickness of the tested specimens was approximately 6 mm, which was the result of stacking three injection-molded plates. Indentation time was 3 s.

The compression set of the samples was determined according to Method A of ISO 815-1:2019. Circular Type B specimens with a diameter of 13 mm and a nominal thickness of 6 mm were compressed by 25% of their initial thickness. To determine the compression set at room temperature, we compressed the specimens at 25 °C for 72 h. For the elevated-temperature test, the compressed specimens were placed in a drying oven (Baxter DN 63, Baxter International, Deerfield, USA) at 70 °C for 24 h. After the exposure period, the compression device was removed from the oven, the load was released, and the specimens were placed on a wooden surface. After a 30 min recovery period, specimen thickness was measured again. The reported compression set values are the average of those of five specimens for each condition.

The rheological behavior of the samples was characterized with a Kinexus Prime Pro+ rotational rheometer (Netzsch Group, Selb, Germany). Oscillatory tests were carried out in a parallel-plate geometry with the use of 25 mm-diameter plates with a 1 mm gap at 190 °C. To determine the linear viscoelastic region (LVER), we performed strain amplitude sweep tests over a strain range of 0.01–150% at a constant frequency of 1 Hz. Based on the identified LVER, frequency-sweep tests were subsequently conducted over the range 0.01–100 Hz at a constant strain of 0.5%.

The morphology of the blends was characterized with a JEOL JSM-6380LA scanning electron microscope (SEM) (JEOL Ltd., Tokyo, Japan). Fracture surfaces obtained after tensile testing were sputter-coated with a thin layer of gold prior to SEM observation.

3. Results and discussion

3.1. Characterization of the rubber phases

Figure 1 shows the thermogravimetric (TGA) and derivative thermogravimetric (dTG) curves of GTR and dGTR. The thermal degradation of both samples occurred in several stages. The mass loss below 150 °C was mainly caused by moisture. Between 150 and 290 °C, low-molecular-weight additives and processing oils were released or decomposed. Natural rubber (NR) degraded mainly between 290 and 400 °C, followed by the degradation of the synthetic rubber components, mainly styrene-butadiene rubber (SBR) and/or butadiene rubber (BR), up to about 590 °C [25, 26]. In air, carbon black oxidized between 600 and 660 °C. The residue above 660 °C was assigned to the inorganic components of the rubber. The temperature corresponding to 5% mass loss ($T_{5\%}$) increased after devulcanization, while the proportion of volatile components decreased (Figure 1 and Table 5). This change can be explained with the partial decomposition and removal of processing oils and low-molecular-weight additives during thermomechanical devulcanization [25, 27]. Minor differences in the composition of the samples may also arise from the heterogeneous origin of waste tires. Tire manufacturers use different proprietary compound formulations, and both GTR and the resulting dGTR are produced from mixtures of tires with different compositions.

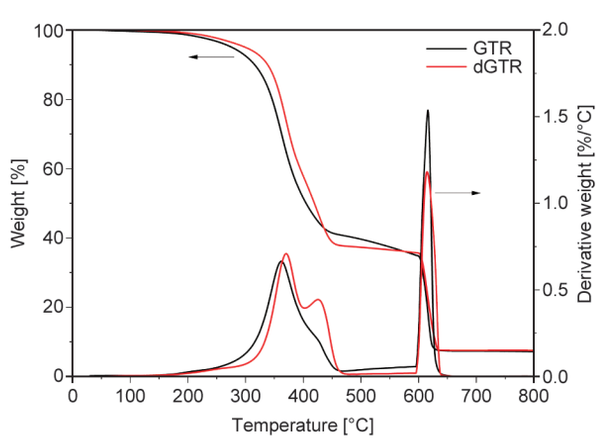

Figure 1. TGA and dTG curves of GTR and dGTR.

Table 5. The result of the TGA test.

Sample	$T_{5\%}$ [°C]	Volatile ingredients		Natural rubber		Synthetic rubber		Carbon black		Residue [%]
		Δm [%]	T_{max} [°C]	Δm [%]	T_{max} [°C]	Δm [%]	T_{max} [°C]	Δm [%]	T_{max} [°C]	
GTR	278.2±3.2	6.1±0.3	–	40.3±1.7	364.6±1.8	16.5±0.3	–	30.9±2.2	617.8±1.8	6.2±1.0
dGTR	300.0±4.5	4.4±0.2	–	38.5±1.2	372.3±1.3	21.4±1.2	429.0±3.3	30.0±1.3	614.3±1.2	5.8±1.2

The degradation peaks assigned to natural and synthetic rubber were more clearly separated in the dGTR sample. This may be related to polymer chain scission and crosslink cleavage during devulcanization, which reduced the connectivity between the different rubber components and allowed their thermal degradation processes to occur more independently. Thermomechanical devulcanization decreased the crosslink density of GTR by approximately 67% and increased the soluble content from 7.6 to 27.4% (Table 6). These changes show that the crosslinked network was extensively degraded during devulcanization. In our previous study [21], Horikx's analysis showed that random polymer chain scission was the main mechanism of the applied devulcanization process rather than selective crosslink cleavage. However, the remaining crosslink density indicates that devulcanization was incomplete, as evidenced by the presence of rubber particles still visible in the dGTR. This is supported by optical microscope images of the polished surfaces of TPU-based blends containing equal amounts (50 wt%) of GTR and dGTR (Figure 2). The 200× magnification clearly shows how the size and quantity of large particles in the rubber phase decreased as a result of devulcanization. The increase in soluble content can therefore be linked to the formation of extractable polymer chains and fragments of low molecular weight.

Table 6. The crosslink density and soluble content of the rubber phases.

Sample	Crosslink density, v_e [mol/cm^3·10^{-4}]	Soluble content, S [%]
GTR	3.78±0.16	7.6±0.4
dGTR	1.25±0.04	27.4±1.3
dGTR-S	2.51±0.07	11.5±0.8
dGTR-P	2.16±0.03	10.7±0.4

Revulcanization with sulfur- and peroxide-based vulcanization systems increased crosslink density and reduced the soluble content of dGTR. However, the original crosslink density of GTR could not be restored with either vulcanization system. This can be explained with the irreversible polymer chain scission during thermomechanical devulcanization. The broken polymer chains cannot be reconnected during revulcanization, therefore the newly formed crosslinks cannot fully rebuild the original three-dimensional network.

3.2. Vulcanization characteristics of the rubber compounds

The vulcanization behavior of the rubber compounds provides useful information for understanding the

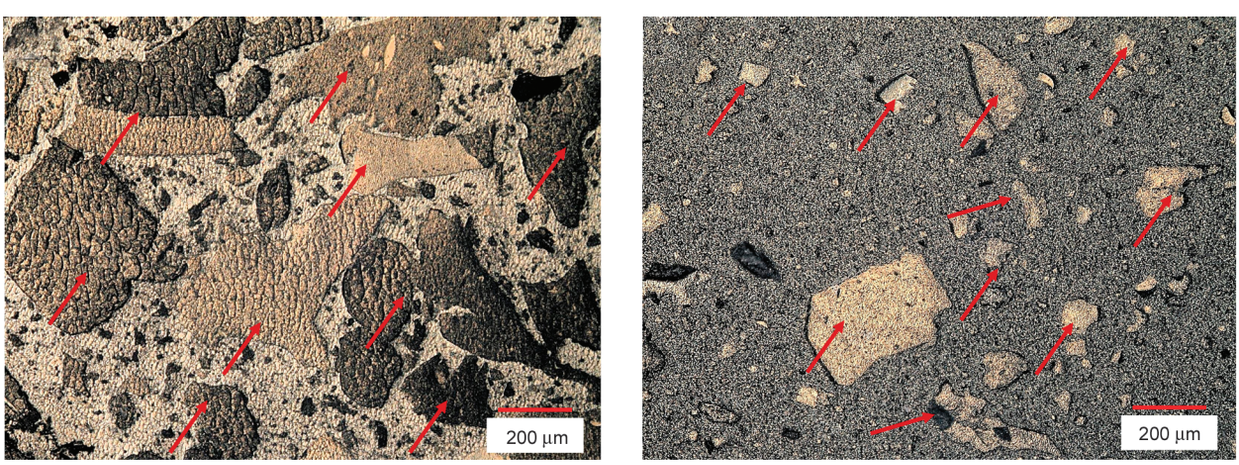

a) b)

Figure 2. The optical microscope image (200× magnification) of the polished surface of a sample containing 50 wt% of a) GTR and b) dGTR.

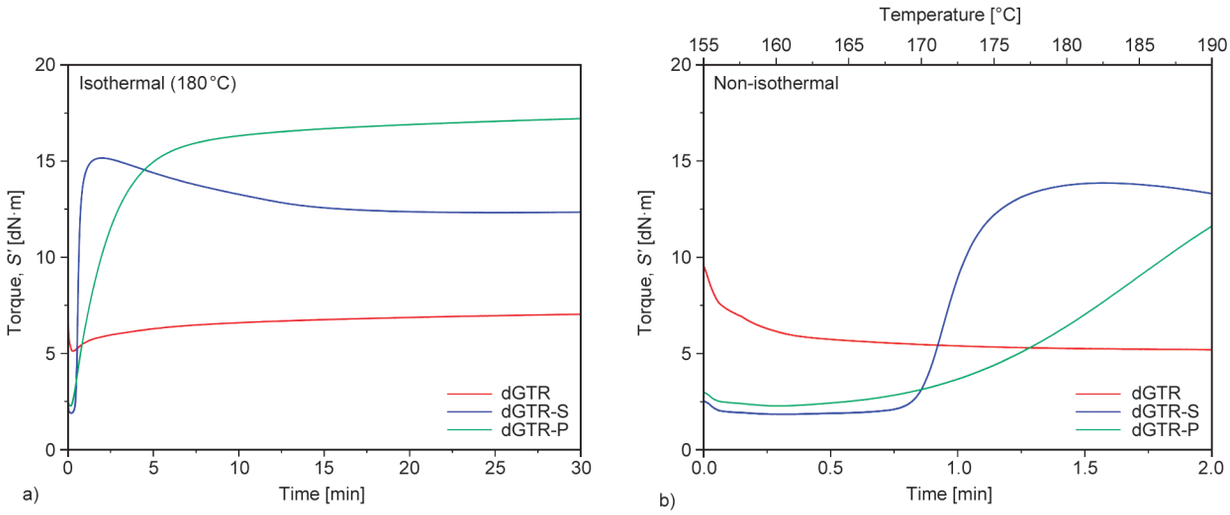

Figure 3. a) Isothermal (180 °C) and b) non-isothermal vulcanization curves for the rubber phases.

Table 7. Vulcanization characteristics of the rubber compounds.

Sample	Temperature [°C]	$S'_{max} - S'_{min}$ [dN·m]	*CRI* [1/min]	t_{10} [min]	t_{90} [min]
dGTR	180	1.9	5.5	0.6	18.8
	155→190 (17.5 °C/min)	Cannot be determined			
dGTR-S	180	13.3	243.9	0.5	0.9
	155→190 (17.5 °C/min)	12.0	294.1	0.8	1.2
dGTR-P	180	13.4	16.4	0.5	6.6
	155→190 (17.5 °C/min)	9.2	Cannot be determined		

development of the rubber phase during dynamic vulcanization and its effect on the final properties of thermoplastic dynamic vulcanizates (TDVs). Therefore, we tested neat dGTR and sulfur- (dGTR-S) and peroxide-based (dGTR-P) rubber compounds under isothermal (180 °C) and non-isothermal conditions (Figure 3 and Table 7).

Neat dGTR showed only a small increase in torque ($\Delta S'$ = 1.91 dNm) during the isothermal test and had a low cure rate (*CRI* = 5.49 min^{-1}). This shows that the residual vulcanization agents in dGTR have limited activity and can only form a small number of new crosslinks. Under non-isothermal conditions, which followed the temperature profile used during TDV processing, there was almost no increase in torque. Therefore, the residual vulcanization agents in dGTR cannot form a significant number of new crosslinks during extrusion. Both rubber compounds containing added vulcanization agents (dGTR-S and dGTR-P) showed a clear increase in torque due to crosslink formation. Under isothermal conditions, dGTR-S and dGTR-P showed similar maximum torque differences, but their vulcanization rates differed significantly. The sulfur-based compound vulcanized rapidly, reaching optimum cure in 0.9 min. In comparison, the peroxide-based compound required 6.6 min to reach the same degree of vulcanization.

The non-isothermal curves provided more information about the vulcanization of the rubber phase during extrusion. By the end of the test, the torque of dGTR-S had approached a plateau, showing that vulcanization could be completed within a timeframe comparable to the extrusion residence time. The torque of the dGTR-P continued to increase after 2 min, indicating that the peroxide-based vulcanization reaction was unlikely to be completed during extrusion alone. However, dGTR-P passed the scorch time (t_{10}) within this period. The dispersed rubber particles therefore had sufficient network integrity to prevent coalescence within the TPU melt, which is required for dynamic vulcanization. During injection molding, the material was exposed to a higher melt temperature of 210 °C, which allowed the peroxide-based vulcanization reaction to continue.

3.3. Tensile behavior of the blends

Figure 4 shows typical tensile stress–strain curves, while Figure 5 summarizes tensile strength and elongation at break as a function of rubber content. Neat TPU had a tensile strength of approximately 22 MPa and an elongation at break of about 890%. Gradually

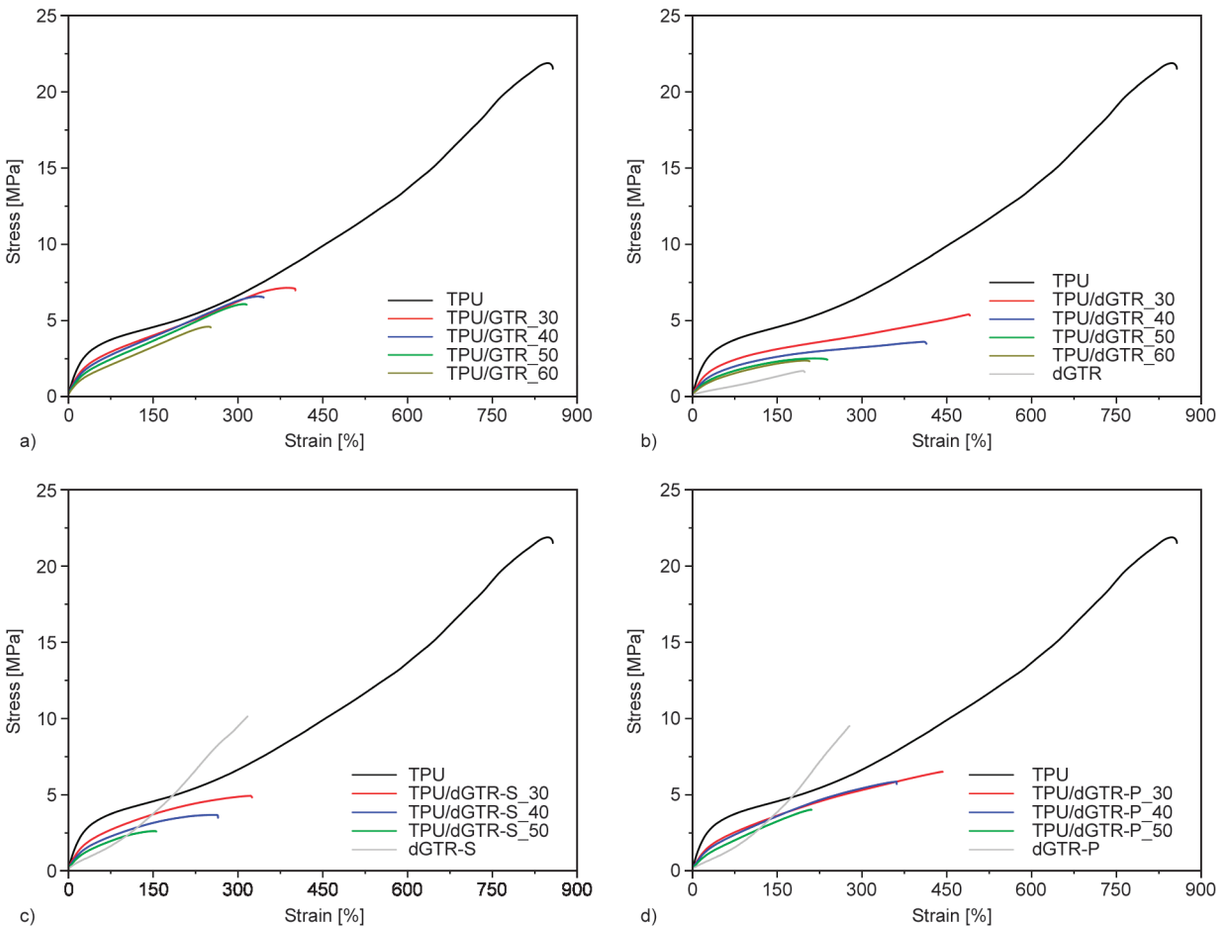

Figure 4. Typical tensile curves of the matrix TPU and blends: a) TPU/GTR, b) TPU/dGTR, c) TPU/dGTR-S, d) TPU/dGTR-P.

increasing the rubber content reduced both properties in all blends. This can be explained with a mechanically weaker rubber phase, and reduced *stress transfer between the two phases*.

The rubber phase also changed the shape of the tensile curves. Neat TPU showed a clear plateau between approximately 50 and 200% strain, which has been linked to microstructural rearrangements in the phase-separated TPU morphology. At higher strains, molecular chain orientation resulted in pronounced strain hardening [28–30]. In the GTR-filled blends, the plateau and strain-hardening

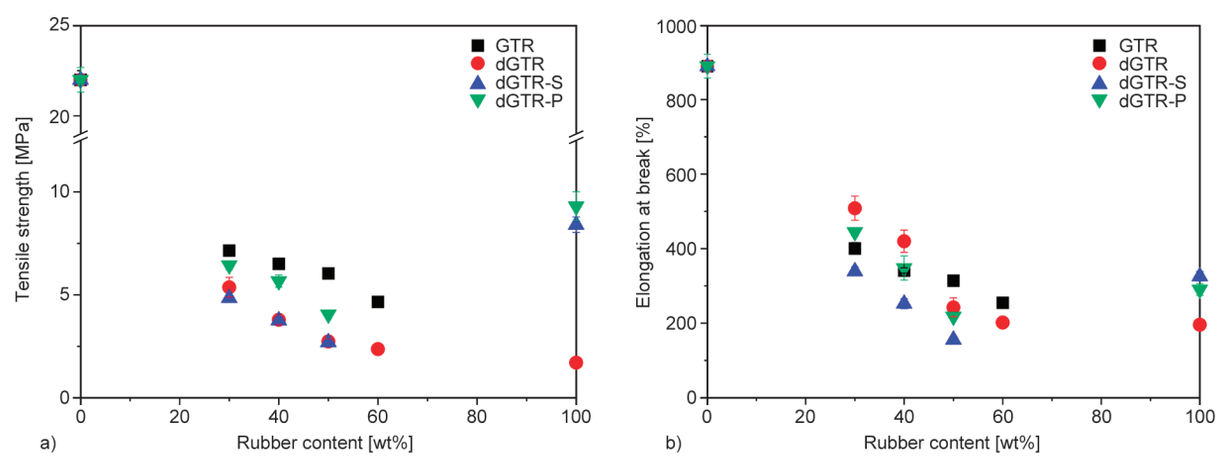

Figure 5. a) Tensile strength and b) elongation at break as a function of rubber content.

regions gradually became less pronounced. Both features almost completely disappeared in the dGTR-containing blends. As the rubber content increases, less TPU is available for microstructural rearrangement and strain hardening. At the same time, the dispersed rubber particles restrict molecular orientation and structural rearrangement in the TPU matrix. This effect was stronger in the blends containing dGTR.

At the same rubber content, the GTR-filled blends had higher tensile strength than the blends containing dGTR. This difference is consistent with the partial breakdown of the crosslinked network and polymer chain scission during devulcanization. However, up to 40 wt% rubber content, the blends containing dGTR had higher elongation at break than the corresponding GTR-filled blends. The increased chain mobility and changes in surface chemistry caused by devulcanization may enhance interactions between the TPU matrix and the rubber phase, as reported in previous studies [9, 31, 32].

The TDVs (TPU/dGTR-S and TPU/dGTR-P) showed a similar trend. Tensile strength and elongation at break decreased as rubber content increased, and the plateau and strain-hardening regions of neat TPU disappeared. At the same rubber content, the peroxide-cured blends had higher tensile strength and elongation at break than the sulfur-cured blends. Peroxide-based dynamic vulcanization may enhance interactions between the TPU matrix and the rubber phase, enabling more efficient stress transfer and improved mechanical performance [33]. Additionally, it cannot be excluded that the peroxide-based vulcanization system affects the TPU matrix as well.

The tensile properties of the TDVs were worse than those of the separately vulcanized dGTR-S and dGTR-P compounds, even though the latter formed continuous crosslinked rubber networks. In the TDVs, the rubber phase was dispersed within the TPU matrix, and the mechanical response was therefore controlled by stress transfer between the phases, local stress concentration, and possible phase separation during deformation. At the same time, the increasing rubber content reduced the amount of continuous TPU available for molecular orientation and strain hardening. These effects explain why the tensile properties of the blends did not follow a simple rule of mixtures and could remain below those of both neat TPU and the separately vulcanized rubber compounds.

Two-way ANOVA showed that rubber type or vulcanization system, rubber content, and their interaction had significant effects on both tensile strength and elongation at break ($p < 0.05$). Tukey's post hoc test confirmed that the GTR-filled blends had significantly higher tensile strength than the corresponding dGTR-containing blends at all rubber contents. The elongation at break of the dGTR-containing blends was significantly higher at 30 and 40 wt% rubber content, while the opposite trend was found at 50 and 60 wt%. Among the thermoplastic dynamic vulcanizates, the peroxide-cured blends had significantly higher tensile strength and elongation at break than the sulfur-cured blends at all investigated rubber contents.

3.4. The hardness and compression set of the blends

Figure 6 shows the Shore A hardness of the blends. Hardness gradually decreased as rubber content increased across all blends. The blends containing dGTR had the largest decrease, while the hardness of the thermoplastic dynamic vulcanizates (TDVs) was between that of the GTR- and dGTR-containing blends. This trend is consistent with the crosslink density results presented in Section 3.1. Devulcanization reduced the stiffness of the rubber phase, while dynamic revulcanization partially restored it.

The compression set of the blends was measured at 25 and 70 °C (Figure 7). The addition of the rubber phase slightly increased compression set at both

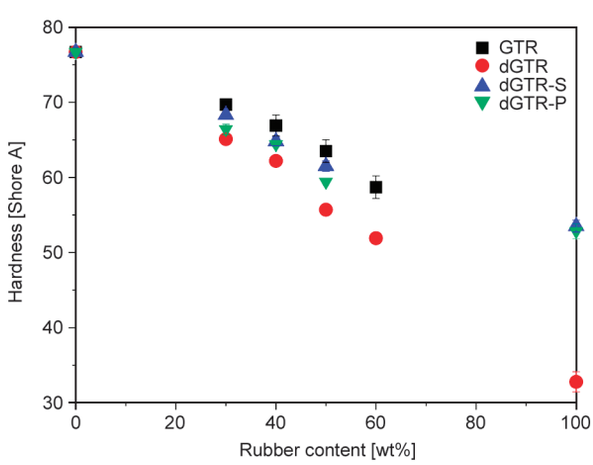

Figure 6. Shore A hardness of the samples as a function of rubber content.

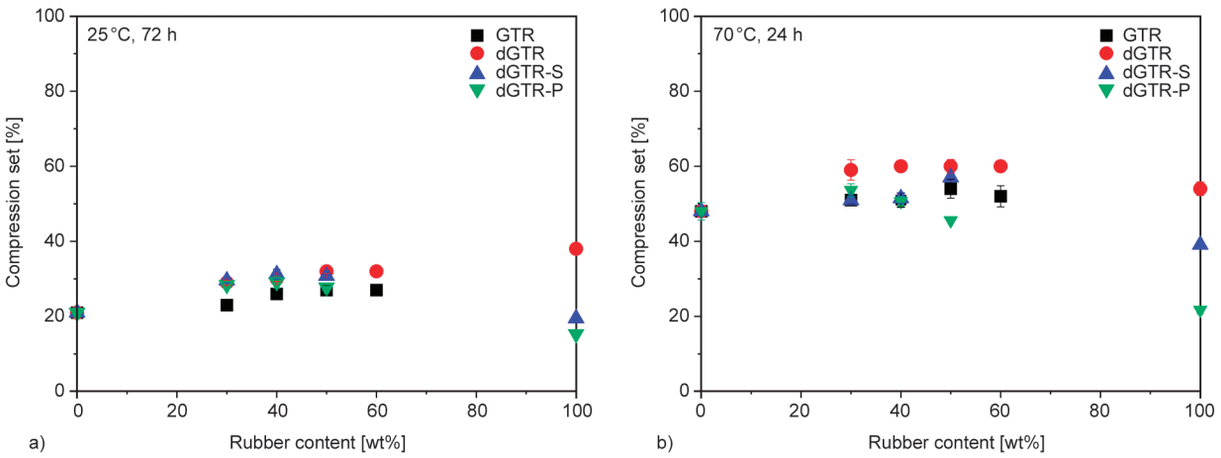

Figure 7. Compression set of the samples at a) 25 °C and b) 70 °C as a function of rubber content.

temperatures compared with neat TPU, but the effect of increasing rubber content was small. The blends containing dGTR had the highest compression set values, which is consistent with the lower crosslink density of dGTR.

The lower Shore A hardness and higher compression set of the GTR-filled blends compared with neat TPU cannot be explained only by the mechanical properties of the rubber particles.The Shore A hardness of truck tire tread compounds is comparable to that of the TPU used in this study. Therefore, the TPU–rubber interphase may also have an important role in the mechanical response of the blends. This agrees with the conclusions drawn from the tensile test results.

The compression set of the TDVs was only slightly higher than that of neat TPU. The peroxide-cured blends had lower compression set values, especially at 70 °C. At this temperature, the compression set of the blend containing 50 wt% dGTR-P was close to that of neat TPU. The lower compression set of the peroxide-cured blends may be related to changes in the TPU–rubber interphase that allow more efficient stress transfer, or it may be due to the effect of the peroxide-based vulcanization system on the TPU matrix.

Shore A hardness and compression set were affected by both the crosslink density of the rubber phase and the TPU–rubber interphase. Dynamic revulcanization, especially with the peroxide-based vulcanization system, partly compensated for the reduction in mechanical performance observed in the dGTR-containing blends. This was also reflected in the higher tensile strength and elongation at break and the lower compression set of the peroxide-cured blends.

3.5. Rheological behavior of the blends

We determined the linear viscoelastic region (LVER) of the blends based on the amplitude dependence of the storage modulus (G') (Figure 8) and selected a strain amplitude of 0.5% for the following oscillatory tests, as it was within the LVER of all samples.

The storage modulus increased with increasing rubber content across all blends, indicating that the rubber phase enhanced the elastic response of the melt. At the same rubber content, the blends containing dGTR had higher G' values than the corresponding GTR-filled blends. This difference may be related to the higher chain mobility of dGTR and the resulting changes in the interactions within the melt. The thermoplastic dynamic vulcanizates showed a similar increase in G' with rubber content, indicating that the dynamically vulcanized rubber phase also increased the elasticity of the melt.

G' gradually decreased with increasing strain amplitude for all samples. This Payne effect–like behavior became more pronounced as rubber content increased due to the gradual breakdown of the particle network during deformation. The blends containing dGTR showed a larger decrease in modulus than the GTR-filled blends, which may be related to the greater structural rearrangement of the network formed by the devulcanized rubber particles. Among the thermoplastic dynamic vulcanizates, the peroxide-cured blends showed a smaller decrease in G' than the sulfur-cured blends. The melt structure of the peroxide-cured blends therefore appeared to be less sensitive to structural rearrangement during deformation.

Figure 9 and Figure 10 show the frequency dependence of the storage modulus (G') and complex

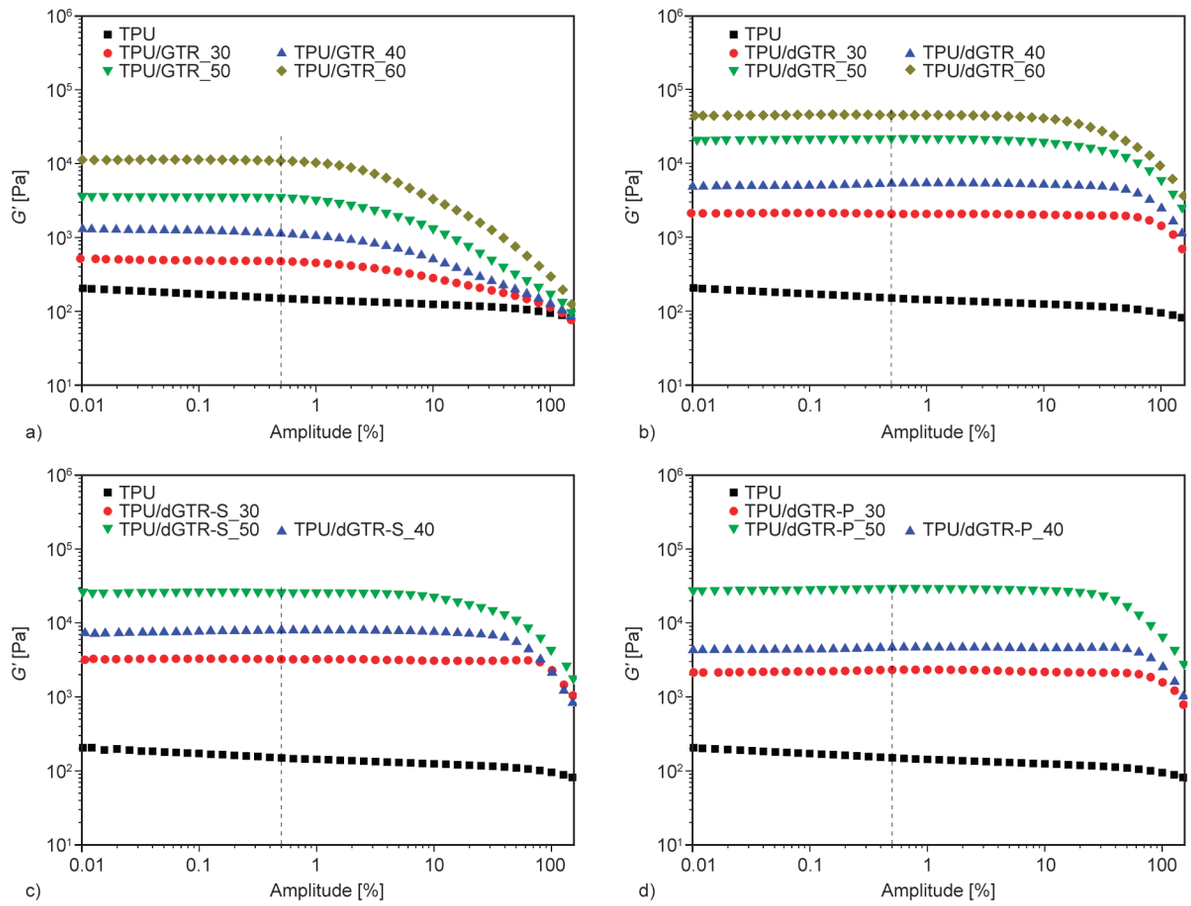

Figure 8. The storage modulus (G') of samples containing a) GTR, b) dGTR, c) dGTR-S and d) dGTR-P as a function of amplitude.

viscosity (η^*). All blends exhibited the typical viscoelastic behavior of polymer melts: G' increased and η^* decreased with increasing frequency. The rubber phase clearly affected the rheological behavior of the blends. Both G' and η^* increased with rubber content, especially at low frequencies. At the same time, G' became less frequency-dependent, which is consistent with more restricted long-term relaxation and a stronger elastic response of the melt. At the same rubber content, the blends containing dGTR had higher G' and η^* values than the corresponding GTR-filled blends over the entire frequency range. This agrees with the amplitude-sweep results and may be related to structural changes caused by devulcanization, which increase chain mobility and alter the behavior of the rubber phase in the melt. The effect of the rubber phase was strongest at low frequencies. As the frequency increased, the complex viscosity curves gradually approached one another. At high deformation rates, the flow behavior of the TPU matrix therefore became more dominant.

The thermoplastic dynamic vulcanizates showed the same general trend. Both G' and η^* increased with rubber content, while their frequency dependence decreased. There were only small differences between the sulfur- and peroxide-cured blends. Among the studied compositions, rubber content had a greater effect on melt rheology than the vulcanization system did.

3.6. The morphology of the blends

Figure 11 shows representative SEM micrographs of the tensile fracture surfaces of neat TPU and the blends containing 40 wt% recycled rubber. The fracture surface of neat TPU (Figure 11a) is relatively smooth and homogeneous, which is characteristic of the ductile fracture of the TPU matrix. In contrast, all rubber-filled blends exhibit rougher fracture surfaces with visible rubber particles and cavities

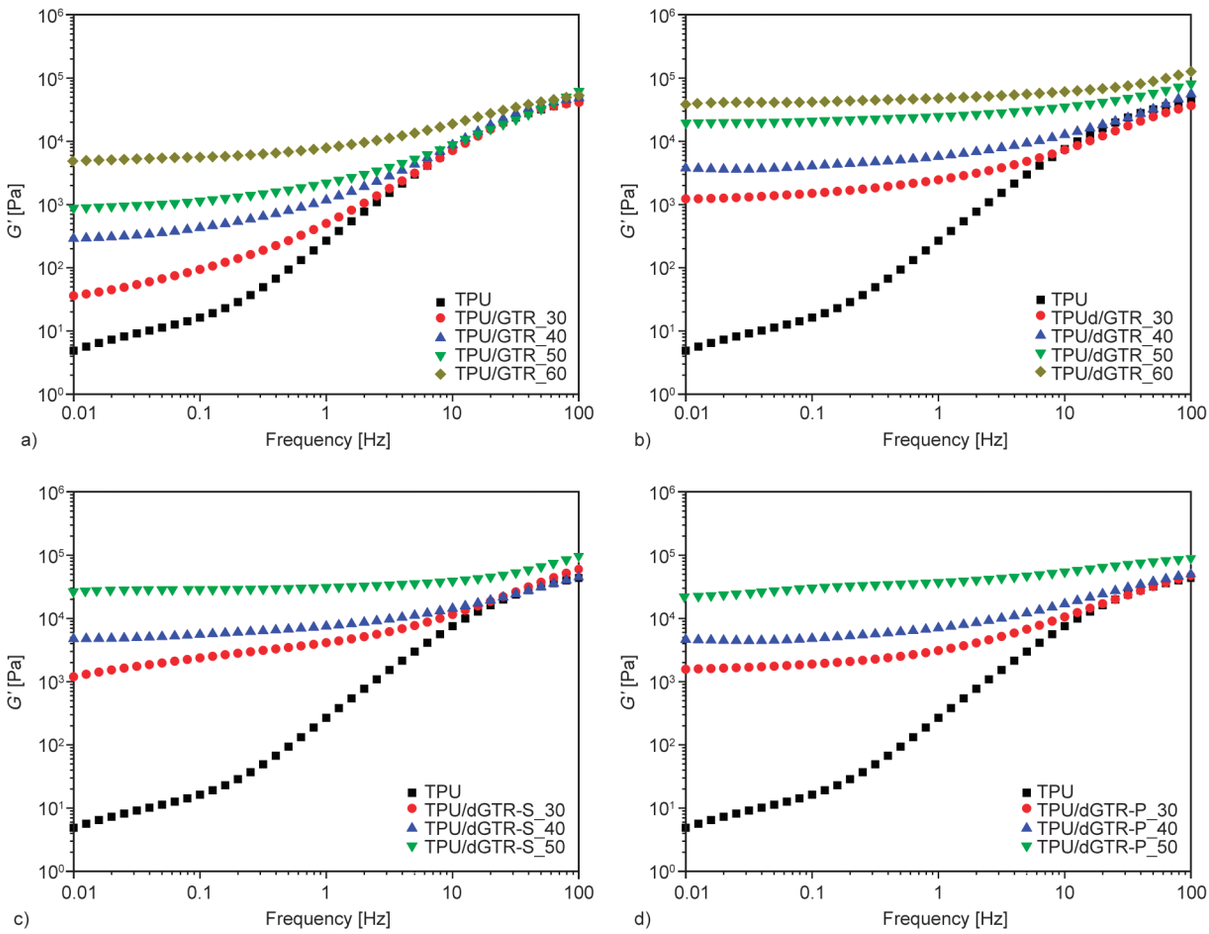

Figure 9. Storage modulus (*G'*) of samples containing a) GTR, b) dGTR, c) dGTR-S and d) dGTR-P as a function of frequency.

resulting from the separation of interfaces and particle pull-out.

The TPU/GTR blend (Figure 11b) contains numerous cavities and detached rubber particles, indicating interfacial debonding during tensile loading. The TPU/dGTR blend (Figure 11c) shows a rougher fracture surface than the corresponding GTR-filled blend, suggesting a different fracture mechanism that is consistent with its higher elongation at break. Dynamic vulcanization further changed the fracture morphology of specimens with 40 wt% rubber content (Figure 11d and Figure 11e). Compared with the TPU/dGTR blend, the fracture surfaces of the dynamically vulcanized blends appear more continuous and contain fewer large cavities. Only minor morphological differences can be observed between the sulfur- and peroxide-cured blends. Overall, the SEM observations support the mechanical and rheological results and demonstrate that the structural state of the recycled rubber phase clearly affects the fracture behavior of the TPU-based blends.

4. Conclusions

In this study, we compared the effect of ground tire rubber (GTR), devulcanized ground tire rubber (dGTR) and dynamically vulcanized dGTR on the mechanical and rheological properties of TPU-based blends. The lower crosslink density and higher soluble content of dGTR confirmed the extensive changes in the rubber network caused by devulcanization. Revulcanization with sulfur- and peroxide-based vulcanization systems increased the crosslink density of dGTR, but the original network structure of GTR could not be fully restored.

The rubber phase clearly affected the mechanical properties of the blends. At the same rubber content, the GTR-filled blends had higher tensile strength than the blends containing dGTR. However, up to

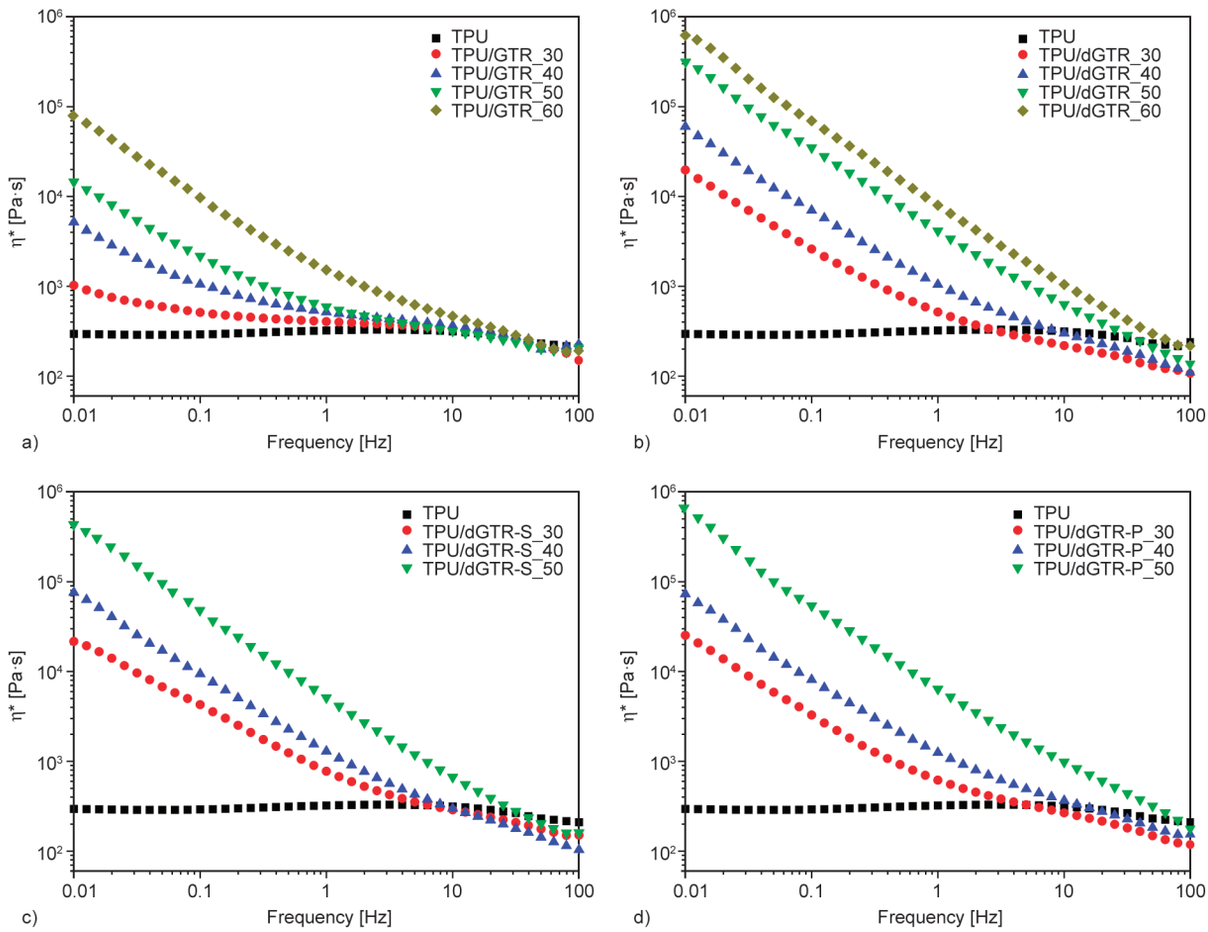

Figure 10. The complex viscosity (η^*) of samples containing a) GTR, b) dGTR, c) dGTR-S and d) dGTR-P as a function of frequency.

40 wt% rubber content, the blends containing dGTR had higher elongation at break. The thermoplastic dynamic vulcanizates showed intermediate behavior between the GTR- and dGTR-filled blends. Among the dynamically vulcanized blends, the peroxide-cured samples had higher tensile strength and elongation at break and lower compression set than the sulfur-cured samples. These results are consistent with improved stress transfer between the TPU matrix and the peroxide-cured rubber phase, although a possible contribution from changes in the TPU matrix cannot be excluded.

The rheological results also showed clear differences between GTR and dGTR. The blends containing dGTR had higher storage modulus (G') and complex viscosity (η^*) than the corresponding GTR-filled blends. Increasing the rubber content increased the elastic response of the melt and reduced the frequency dependence of G'. The sulfur- and peroxide-cured blends showed only small differences in melt rheology, showing that rubber content had a greater effect on melt behavior than the vulcanization system.

The results show that both the amount and structure of recycled tire rubber strongly affect the properties of TPU/rubber blends. Devulcanization alters the mechanical and rheological behavior of the rubber phase, while subsequent dynamic vulcanization partly compensated for the changes observed in the mechanical properties of the dGTR-containing blends. The choice of vulcanization system is especially important for the mechanical properties of the thermoplastic dynamic vulcanizates. These findings show that controlling the structure of the recycled rubber phase can be used to adjust the properties of TPU blends and support the high-value use of end-of-life tire rubber.

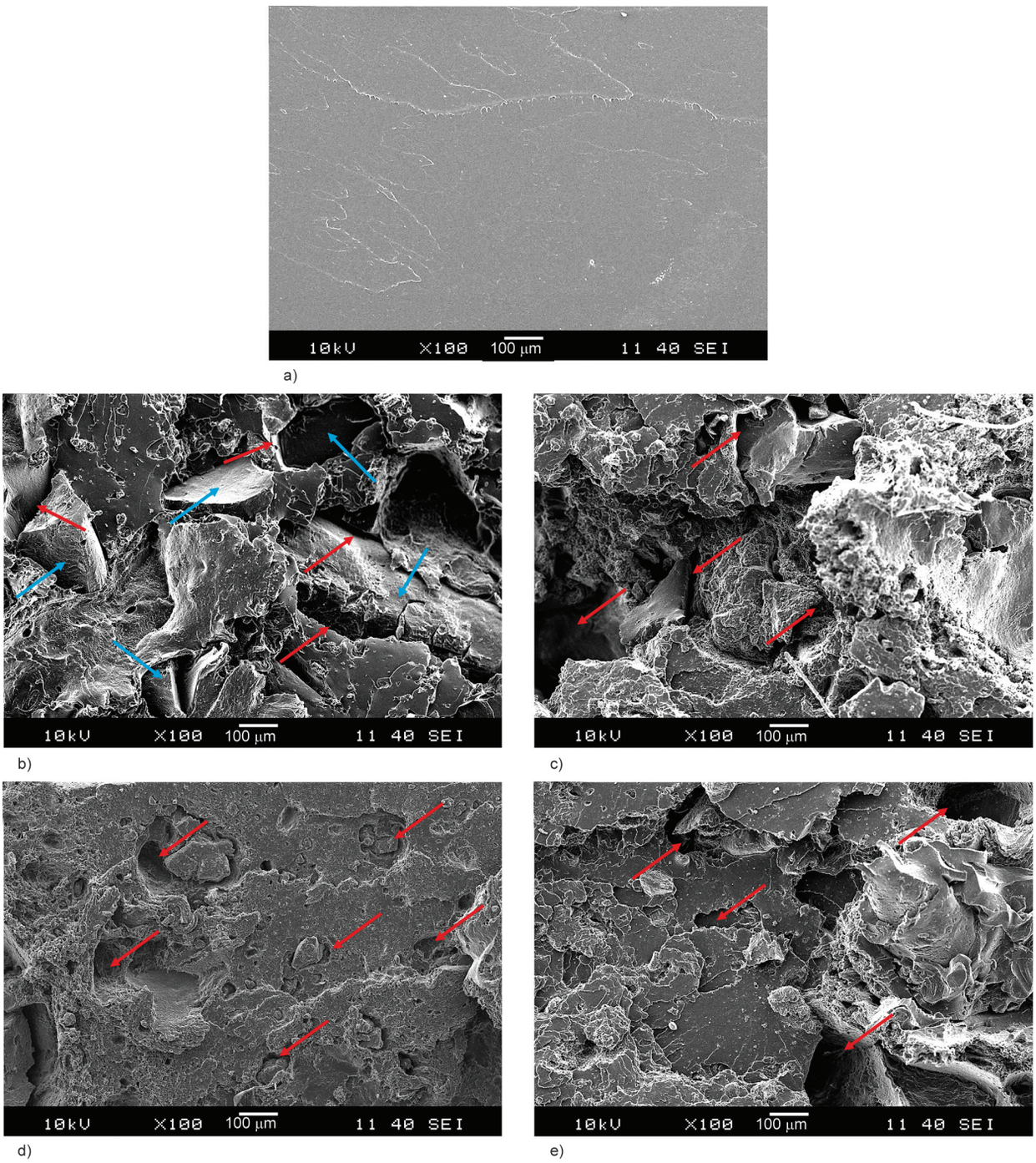

Figure 11. Representative SEM micrographs of tensile fractured surfaces of neat TPU and specimens with 40 wt% rubber content: a) TPU, b) TPU/GTR_40, c) TPU/dGTR_40, d) TPU/dGTR-S_40 and e) TPU/dGTR-P_40.

Acknowledgements

This research was funded by the National Research, Development and Innovation Office, Hungary (K 128268 and K 146085). Project HERO was selected in the Joint Transnational Call 2022 of M-ERA.NET 3, which is an EU-funded network of about 49 funding organisations (Horizon 2020 grant agreement No 958174). The project was implemented with the support of the Ministry of Culture and Innovation of Hungary from the National Research, Development and Innovation Fund, on the basis of a grant document issued by the National Research, Development and Innovation Office (2023-1.2.1-ERA_NET-2023-00003).

References

[1] Saputra R., Walvekar R., Khalid M., Mubarak N. M., Sillanpää M.: Current progress in waste tire rubber devulcanization. Chemosphere, **265**, 129033 (2021). https://doi.org/10.1016/j.chemosphere.2020.129033

[2] Laftah W. A., Wan Abdul Rahman W. A.: A comprehensive review of tire recycling technologies and applications. Materials Advances, **6**, 4992–5010 (2025). https://doi.org/10.1039/d5ma00463b

[3] Dabic-Miletic S., Simic V., Karagoz S.: End-of-life tire management: A critical review. Environmental Science and Pollution Research, **28**, 68053–68070 (2021). https://doi.org/10.1007/s11356-021-16263-6

[4] Karger-Kocsis J., Mészáros L., Bárány T.: Ground tyre rubber (GTR) in thermoplastics, thermosets, and rubbers. Journal of Materials Science, **48**, 1–38 (2013). https://doi.org/10.1007/s10853-012-6564-2

[5] Ramarad S., Khalid M., Ratnam C. T., Chuah A. L., Rashmi W.: Waste tire rubber in polymer blends: A review on the evolution, properties and future. Progress in Materials Science, **72**, 100–140 (2015). https://doi.org/10.1016/j.pmatsci.2015.02.004

[6] Formela K.: Strategies for compatibilization of polymer/waste tire rubber systems prepared *via* melt-blending. Advanced Industrial and Engineering Polymer Research, **7**, 466–481 (2024). https://doi.org/10.1016/j.aiepr.2023.08.001

[7] Srisuwanno T., Johns J., Bascucci C., Clemens F., Nakaramontri Y.: Effect of bio-based epoxidized natural rubber as a compatibilizer in thermoplastic polyurethane/natural rubber blends: Physical characterization and 3D printing behavior. Express Polymer Letters, **19**, 1053–1072 (2025). https://doi.org/10.3144/expresspolymlett.2025.79

[8] Kohári A., Bárány T.: The growth and recyclability of thermoplastic polyurethanes. Express Polymer Letters, **18**, 459–460 (2024). https://doi.org/10.3144/expresspolymlett.2024.33

[9] Kohári A., Bárány T.: Sustainable thermoplastic elastomers based on thermoplastic polyurethane and ground tire rubber. Journal of Applied Polymer Science, **141**, e56157 (2024). https://doi.org/10.1002/app.56157

[10] Formela K., Cieslik M.: Ground tire rubber in the sustainable development of flexible and conductive thermoplastic polyurethane/carbon black composites. Polymers, **18**, 741 (2026). https://doi.org/10.3390/polym18060741

[11] Kyriakidis I. F., Kladovasilakis N., Korlos A., Tzetzis D., Pechlivani E. M., Tsongas K.: Dynamic-mechanical investigation of thermoplastic polyurethane/ground tire rubber composites through selective laser sintering additive manufacturing. The International Journal of Advanced Manufacturing Technology, **141**, 1987–2006 (2025). https://doi.org/10.1007/s00170-025-16620-6

[12] Markl E., Lackner M.: Devulcanization technologies for recycling of tire-derived rubber: A review. Materials, **13**, 1246 (2020). https://doi.org/10.3390/ma13051246

[13] Yang L., Zhao X., Xinyu S., Yuan S., Zhu L.: Selective devulcanization of ground tire rubber by choline-based deep eutectic solvents for high-performance recycled materials. Express Polymer Letters, **19**, 783–795 (2025). https://doi.org/10.3144/expresspolymlett.2025.60

[14] Simon D. Á., Halász I. Z., Karger-Kocsis J., Bárány T.: Microwave devulcanized crumb rubbers in polypropylene based thermoplastic dynamic vulcanizates. Polymers, **10**, 767 (2018). https://doi.org/10.3390/polym10070767

[15] Wu H., Tian M., Zhang L., Tian H., Wu Y., Ning N.: New understanding of microstructure formation of the rubber phase in thermoplastic vulcanizates (TPV). Soft Matter, **10**, 1816–1822 (2014). https://doi.org/10.1039/c3sm52375f

[16] Bhattacharya A. B., Chatterjee T., Naskar K.: Automotive applications of thermoplastic vulcanizates. Journal of Applied Polymer Science, **137**, 49181 (2020). https://doi.org/10.1002/app.49181

[17] Görbe Á., Marton G. Zs., Bárány T.: The effect of transpolyoctenamer on thermoplastic dynamic vulcanizates from devulcanized ground tire rubber and polypropylene. ACS Omega, **11**, 37936–37946 (2026). https://doi.org/10.1021/acsomega.6c03249

[18] Halász I. Z., Kocsis D., Simon D. Á., Kohári A., Bárány T.: Development of polypropylene-based thermoplastic elastomers with crumb rubber by dynamic vulcanization: A potential route for rubber recycling. Periodica Polytechnica Chemical Engineering, **64**, 248–254 (2020). https://doi.org/10.3311/PPch.13962

[19] Punnarak P., Tantayanon S., Tangpasuthadol V.: Dynamic vulcanization of reclaimed tire rubber and high density polyethylene blends. Polymer Degradation and Stability, **91**, 3456–3462 (2006). https://doi.org/10.1016/j.polymdegradstab.2006.01.012

[20] Datta J., Włoch M.: Morphology and properties of recycled polyethylene/ground tyre rubber/thermoplastic poly(ester-urethane) blends. Macromolecular Research, **23**, 1117–1125 (2015). https://doi.org/10.1007/s13233-015-3155-5

[21] Görbe Á., Kohári A., Bárány T.: Rubber compounds from devulcanized ground tire rubber: Recipe formulation and characterization. Polymers, **16**, 455 (2024). https://doi.org/10.3390/polym16040455

[22] Simon D. Á., Bárány T.: Effective thermomechanical devulcanization of ground tire rubber with a co-rotating twin-screw extruder. Polymer Degradation and Stability, **190**, 109626 (2021). https://doi.org/10.1016/j.polymdegradstab.2021.109626

[23] Simon D. Á., Bárány T.: Microwave devulcanization of ground tire rubber and its improved utilization in natural rubber compounds. ACS Sustainable Chemistry and Engineering, **11**, 1797–1808 (2023). https://doi.org/10.1021/acssuschemeng.2c05984

[24] Mangili I., Lasagni M., Anzano M., Collina E., Tatangelo V., Franzetti A., Caracino P., Isayev A. I.: Mechanical and rheological properties of natural rubber compounds containing devulcanized ground tire rubber from several methods. Polymer Degradation and Stability, **121**, 369–377 (2015). https://doi.org/10.1016/j.polymdegradstab.2015.10.004

[25] Garcia P. S., de Sousa F. D. B., de Lima J. A., Cruz S. A., Scuracchio C. H.: Devulcanization of ground tire rubber: Physical and chemical changes after different microwave exposure times. Express Polymer Letters, **9**, 1015–1026 (2015). https://doi.org/10.3144/expresspolymlett.2015.91

[26] Saputra R., Walvekar R., Khalid M., Ratnam C. T., Mubarak N. M., Dharaskar S.: Devulcanisation of ground rubber tyre by novel ternary deep eutectic solvents. Journal of Molecular Liquids, **306**, 112913 (2020). https://doi.org/10.1016/j.molliq.2020.112913

[27] Rodak A., Haponiuk J., Wang S., Formela K.: Waste tire rubber with low and high devulcanization level prepared in the planetary extruder. Sustainable Materials and Technologies, **43**, e01193 (2025). https://doi.org/10.1016/j.susmat.2024.e01193

[28] Miao Y., He H., Li Z.: Strain hardening behaviors and mechanisms of polyurethane under various strain rate loading. Polymer Engineering and Science, **60**, 1083–1092 (2020). https://doi.org/10.1002/pen.25364

[29] Scetta G., Ju J., Selles N., Heuillet P., Ciccotti M., Creton C.: Strain induced strengthening of soft thermoplastic polyurethanes under cyclic deformation. Journal of Polymer Science, **59**, 685–696 (2021). https://doi.org/10.1002/pol.20210060

[30] Singh A., Shivling V. D., Khosla P. K., Saini A., Kumar V., Trigunayak A.: Strain hardening and shock mitigation response of polyurethane under high strain rates. AIP Advances, **11**, 115306 (2021). https://doi.org/10.1063/5.0068403

[31] Zhou H., Duan R., Chen B., Chen N., Lu C., Zhou Z.: Interfacial *co*-crosslinking of devulcanized ground tire rubber and recycled polyurethane towards enhanced mechanical and damping properties. Polymer, **342**, 129380 (2026). https://doi.org/10.1016/j.polymer.2025.129380

[32] Simon D. Á., Pirityi D. Z., Bárány T.: Devulcanization of ground tire rubber: Microwave and thermomechanical approaches. Scientific Reports, **10**, 16587 (2020). https://doi.org/10.1038/s41598-020-73543-w

[33] Pichaiyut S., Vennemann N., Nakason C.: Influence of curing systems on dynamically cured epoxidized natural rubber/thermoplastic polyurethane blends. Journal of Elastomers and Plastics, **47**, 28–51 (2013). https://doi.org/10.1177/0095244313489903